ADVANCED MATERIALS

DOI: 10.1002/adma.200502617

Nanoscale Engineering of Biomaterial Surfaces**

By *Anna Marie Lipski*, *Claude Jaquiery*, *Hoon Choi*, *Daniel Eberli*, *Molly Stevens*, *Ivan Martin*, *I.-Wei Chen*, and *V. Prasad Shastri**

Whereas the characteristic dimension of a mammalian cell is of the order of a few microns, cell-surface structures (receptors, receptor clusters, lamellopodia, filopodia) that are used to sample the external environment and interact with biomaterials are on the order of a few tenths of a nanometer. It is fairly well established that biological events invoked on or around a biomaterial are dictated in part by material surface properties, such as chemistry and topography, which, in turn, have a bearing on cellular functions.[1] Despite the well-accepted notion that the interactions between cell-surface structures and a biomaterial surface alter cell functions (e.g., cell attachment, cell migration, cell division, cell differentiation, and cell–cell interactions), relatively few technologies exist that can engineer a biomaterial surface at the nanoscale. Current material-surface-modification strategies can be broadly classified into two categories: 1) those that strive to change surface chemistry, including chemical etching,[2] plasma treatment,[3] and polymer adsorption;[4] and 2) those that strive to change surface topography, for instance, mechanical roughening,[5] nano- and microindentation, and substrate-templating using a well-defined relief to impart topography by using solvent-casting, electro-deposition, chemical-vapor deposition, or compression-molding processes.[6–8] The limitations of all these approaches are their specificity to a class of material and their inability to effect chemistry and topography predictably in a simultaneous fashion.

We hypothesized that simultaneous modification of surface chemistry and topography may be achieved using functionalized nanoparticles, by exploiting their propensity to self assemble into lattices at a solution/material interface. Here we demonstrate that by using an assembly of silica nanoparticles (NPs), important biomaterial surface characteristics, such as charge, roughness, and chemistry, can be varied in a predictable fashion in a single step. Furthermore, we demonstrate that by functionalizing the NP surface a priori, chemistry and surface roughness of a material surface can be modulated in a single step and independently of one another. Finally, we show that nanoparticle surface modifications enhance the growth and osteogenic differentiation of human-bone-marrow-derived mesenchymal progenitor cells (MPCs), as assessed by the up-regulation of bone sialoprotein mRNA expression; thus opening the door to innovative nanoscale technologies to enhance the performance of metallic orthopedic implants and to control stem-cell differentiation. The simplicity of the paradigm makes it amenable to the modification of a wide variety of substrates with a plethora of surface-bound information. Additionally, NP-based surface modification may find potential applications beyond biomaterials and into the realm of photonics and thin-film assemblies.

We used silica NP as a model system to demonstrate the feasibility of this approach. For our initial studies we used NPs 50 nm in diameter, a length scale of the same order of magnitude as the receptor clusters expressed by cells,[9] and assembled them onto 316-L stainless steel (SS) and Ti foils—two of the most commonly used hard materials in medical devices. Atomic force microscopy (AFM) of the surfaces revealed that, prior to modification, SS and Ti surfaces possessed different degrees of surface roughness (R_q),[10] (2.86 ± 1.64) nm and (5.12 ± 2.13) nm, respectively (probability $p = 0.01$; $p \leq 0.05$ was considered significant in all analyses) (Fig. 1A and B). Upon NP modification, both surfaces exhibited a well-ordered assembly of spherical bodies (Fig. 1C and D) and comparable R_q, (3.04 ± 0.66) nm and (4.02 ± 1.24) nm, respectively ($p = 0.12$).[11] This observation was confirmed by using scanning electron microscopy (SEM), which revealed a highly ordered assembly of NPs on the surface (Fig. 1E). Therefore, one important outcome of surface modification using an ordered assembly of NPs is homogenization of topography.

We assessed the mechanical characteristics of the NP assembly using two different tests: 1) an American Society for Testing and Materials (ASTM) peel test to ascertain the adhesion of the NP assembly to the underlying metal substrate,

[*] Prof. V. P. Shastri, A. M. Lipski, H. Choi, Prof. I.-W. Chen
Department of Materials Science and Engineering
University of Pennsylvania, Philadelphia, PA, 19104 (USA)
E-mail: Prasad.Shastri@vanderbilt.edu
Prof. V. P. Shastri
Department of Biomedical Engineering, Vanderbilt University
5824 Stevenson Center, Nashville, TN 37232 (USA)
C. Jaquiery, D. Eberli, Prof. I. Martin
Departments of Surgery and of Research
University Hospital, 4031 Basel (Switzerland)
M. Stevens
Department of Materials, Imperial College
London, England, SW7 2AZ (UK)

[**] This work was supported in part from grants from the US National Institutes of Health (R24 AI-47739-03), the National Science Foundation, the Nanotechnology Institute through the Ben–Franklin Technology Partners of Northeastern Pennsylvania, Vanderbilt Institute for Integrative Biosystems Research and Education (VIIBRE), and an NSF IGERT Fellowship to AML. The authors wish to thank Nancy Schultz from 3M for kindly providing us with the Ruby Red pressure-sensitive tape in order to carry out the ASTM adhesion tests and Jay Sy for the scanning electron microscope image of the ASTM peel test.

ADVANCED MATERIALS

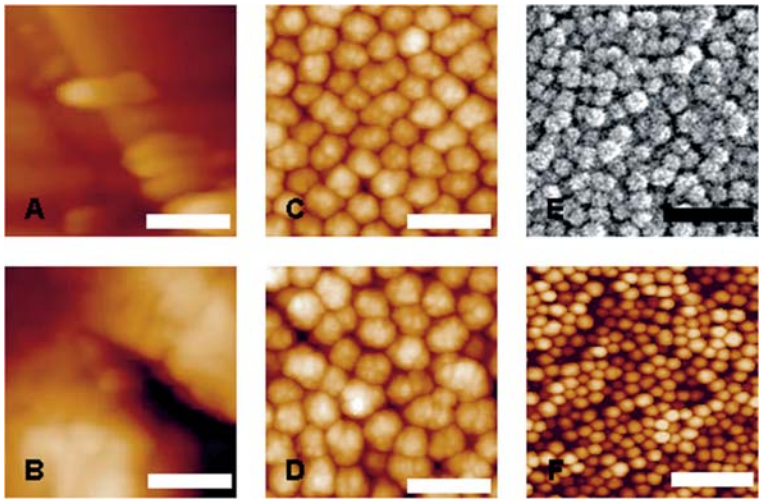

Figure 1. Characterization of NP-modified SS and Ti surfaces: AFM images of unmodified SS (A) and Ti (B), 50 nm NP-modified SS (C) and Ti (D), and 100 nm modified Ti surfaces (F). Scanning electron microscopy (SEM) image of 50 nm NP-modified SS surface (E). Scale bars: A–D 100 nm, E 200 nm, and F 500 nm.

and 2) the resistance of the NP coating to mechanical stresses. The adhesive test was carried out as per ASTM protocol 3395, used for determining adhesion of a coating to a substrate, and the latter was accomplished by indenting the NP particle surface using a diamond AFM tip, details of which are provided as Supporting Information. The NP assembly, remarkably, yielded an adhesion rating of 4 A (trace peeling or removal along incisions) for both Ti and SS surfaces (Fig. 4, Supporting Information). Such a characterization was not possible in the case of polymer substrates as the polymer film itself peeled off along with the adhesive, thus confounding the interpretation of the results. As the coatings on the metal substrates underwent a heat treatment at 80 °C in the oven (and around 40 °C for the polymer samples), formation of covalent bonds between the NP surface hydroxyl groups and the underlying metal oxide layer (which can be expected on the Ti substrate and to a lesser extent on the 316-L SS substrate, in which chromium resides on the surface as an heterogeneous oxide layer (Cr_2O_3)) is a distinct possibility. The nanoindentation studies were consistent with the above findings in that they revealed that the NP coating was quite robust and resistant to shear, compressive, and tensile forces (Fig. 5, Supporting Information). Furthermore, based on the nanoindentation studies we estimated the compressive modulus of the NP coating to be around 52 MPa (Supporting Information). The compressive modulus is at best an estimate, as the porosity of the coating (that is, the porosity of the NP plus the interstitial space between the NPs) confounds the measurement. Based on these results, it is reasonable to conclude that NP assemblies possess some of the prerequisites for implementation as coatings for metallic and polymeric orthopedic devices.

In this paradigm, by varying the NP size the topography can also be varied. Upon modification with 100 nm NPs, both surfaces exhibited increased roughness of (18.63 ± 1.56) nm and (18.11 ± 1.33) nm, respectively (Fig. 1F), which was very reproducible. An important attribute of NP modification is that it can impart predictable roughness to hitherto smooth surfaces. To illustrate this, we investigated spun-cast thin films of nondegradable and degradable soft biomaterials, such as poly(urethane) (data not shown) and poly(L-lactic acid) (PLA), which exhibited smooth morphologies ($R_{q,PLA}$ = (0.22 ± 0.01) nm, Fig. 2A). Upon modification with 50 nm NPs, PLA surfaces showed enhanced roughness of (3.05 ± 0.30) nm (Fig. 2B), which is comparable to modified metal surfaces.[12] By combining well-established patterning techniques such as soft lithography and ink-jet printing[13–15] with NP-based surface modification, one can envision the fabrication of surfaces that exhibit periodicity in chemistry and roughness, which is known to significantly influence cell processes.[16]

We then prefunctionalized silica NPs to bear amine groups (amine-functionalized NPs; ANPs) using aminopropyltriethoxysilane (APS),[17] a well-know silane-coupling agent. The use of APS allowed the presentation of amine functionality, which is the most commonly employed group for tethering biomolecules, at high concentrations under very mild conditions without affecting the NP size.[17,18] This is an important consideration as a high density of information has been shown to favor cell processes, such as adhesion and migration.[19,20] As both silica and ANPs can be obtained as a stable suspension in water, surface modification from an aqueous phase is feasible, which is seldom the case with current surface-modification approaches. The robustness and thickness of the NP assembly on metal surfaces was verified using focused ion beam (FIB) microscopy, which revealed that the NP assembly was several layers thick and was densely packed without any major discontinuities or imperfections (Fig. 1, Supporting Information).

In order to ascertain if functional groups can be presented using a prefunctionalized NP, ANPs were assembled on SS and Ti surfaces and then imaged using AFM. After modifica-

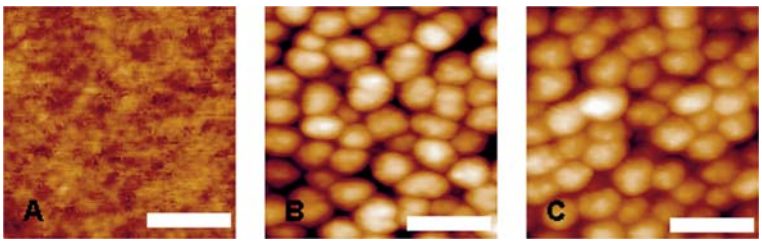

Figure 2. AFM images of: unmodified PLA (A), PLA modified with 50 nm NPs (B), and Ti modified with 50 nm ANPs (C). Scale bar: 100 nm.

tion with ANPs, the R_q of SS and Ti was (4.40 ± 0.67) and (4.73 ± 0.91), respectively, (Ti is shown in Fig. 2C, which is also representative of ANP-modified SS) and was very similar to those previously obtained after modification with underivatized NPs. The concentration of amine groups on these surfaces was determined using a calorimetric assay[21] and was found to be statistically identical at (9.82 ± 2.07) and (10.76 ± 1.94) nmol cm^{-2} on SS and Ti, respectively (p = 0.28). PLA surfaces modified using ANP also exhibited surface roughness (R_q = (4.87 ± 0.93) nm) that was comparable to NP modified surfaces, with amine concentrations ((11.46 ± 1.27) nmol cm^{-2}) similar to those on SS and Ti. In this specific case, ANP modification resulted in the reversal of the charge characteristics[22] of the surface from negative to positive. Such a charge reversal may be leveraged for further surface modification using layer-by-layer adsorption of polyelectrolytes.[23] Yet another important attribute of using NPs to modify surfaces is that the surface chemistry and roughness can be tailored simultaneously but independently of each other. As the chemical conditions involved in the amine-quantification[24] step were identical to those used in the coupling of peptides and proteins to surfaces,[25] the results suggests that amine functionality is chemically accessible and potentially amenable to further modification with biological moieties.

Several studies have suggested that spatial modulation of textural and chemical information can impose beneficial outcomes in cellular functions.[13,26] We cultured murine osteogenic cells, MC-3T3-E1 on modified and unmodified SS and Ti surfaces, and observed that the cell numbers on the NP-modified metal surfaces were either comparable or enhanced (Fig. 2, Supporting Information) over tissue-culture polystyrene (TCPS) controls. Furthermore, cell numbers on SS and Ti modified with ANPs were higher than on NP-modified surfaces. Cell spreading, which can promote a differentiated cell phenotype, was more pronounced on metal and PLA surfaces modified with NPs and ANPs (Fig. 3, Supporting Information). This prompted us to investigate whether surface modification could modulate the growth and lineage-specific differentiation of multipotent progenitor cells. In this respect, one of the most relevant models of the early phases of osteogenic differentiation is based on human-bone-marrow-derived MPCs. Enhancement of MPC differentiation could have potential consequences for the development of osteogenic coatings for orthopedic implants because it is one of the envisioned applications for NP-based surface modification.

Osteogenic differentiation in MPC was induced using osteogenic supplements and the mRNA expression of bone sialoprotein (BSP), a key protein in the biomineralization process, was followed as a function of time. BSP mRNA expression was previously shown to be a quantitative marker of MPC differentiation into an osteogenic lineage in vitro.[27] Numbers and extent of differentiation of MPC cultured on NP-modified SS and Ti surfaces were compared to those on TCPS and sandblasted acid-etched titanium (AET), which is routinely used in dental end-osseous implants. After 14 days of culture, the DNA amounts on the NP-modified metal substrates were significantly higher than those on unmodified surfaces (up to 1.7-fold) or TCPS (up to 2.9-fold), and in the case of modified Ti the values measured approached that of AET (Fig. 3A). As cells adhered with similar efficiencies on different substrates, as assessed by counting nonadherent cells after 24 h (data not shown), higher DNA amounts reflected increased proliferation rates. More importantly, the expression of BSP mRNA (normalized to 18-S ribosomal RNA) in MPC cultured on NP-modified surfaces was an order of magnitude greater than on both the unmodified metals and the TCPS control, and approached that measured on AET (Fig. 3B). However, only a moderate increase in the differentiation capacity of MPC was observed when cultured on ANP-modified SS and Ti surfaces (Fig. 3). As unmodified surfaces were compared to surfaces modified with 50 nm NPs and 50 nm ANPs (comparison pairs: SiO_2–NP:SiO_2–NH_2–NP, SiO_2–NP:AET,

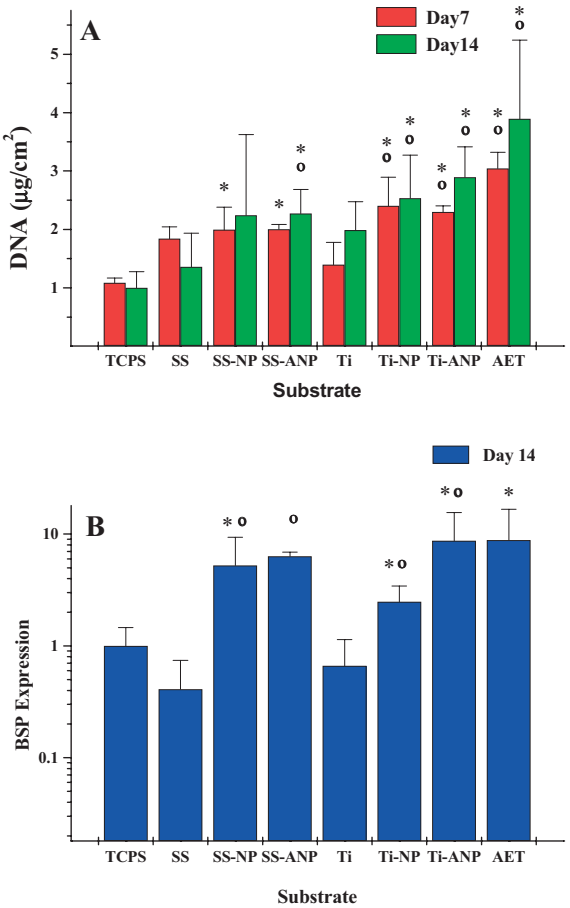

Figure 3. DNA content (A) and mRNA expression levels of bone sialoprotein (BSP) (B) of human-bone-marrow-derived MPCs cultured on the different substrates for up to 14 days. Values are the average of two independent donors and are expressed as fold difference over those measured on TCPS at day 14 using cells from the same donor. Statistically significant differences from TCPS (*) or from the corresponding untreated surface (o) were determined by Mann–Whitney tests (p < 0.05).

ADVANCED MATERIALS

SiO_2–NP:TCPS), this allowed for the decoupling of the surface chemistry from the rugosity and therefore, the observations suggest that MPC differentiation is more influenced by rugosity than by surface charge. This was further borne out by the finding that the mRNA expression on AET was an order of magnitude greater than that on unmodified Ti. As both AET and Ti have the same surface chemistry, which is the presence of an oxide layer, the primary difference between the two surfaces lies in the fact that AET has a rough surface, composed primarily of nanometer-sized pits (created by acid washing; 1–2 μm) interspersed with micrometer-sized features (10–20 μm), conferred by the plasma spraying, attributes that are absent in the case of Ti surfaces studied.

These findings suggest the NP assemblies may be used as a modulator or trigger of osteogenic functions.[28] Past studies have demonstrated nucleation and growth of apatite crystals on silicate classes from simulated body fluid, whereas we have demonstrated cell-driven biomineralization on silicon oxide surfaces. Although protein adsorption cannot be avoided in an in vivo environment, studies under serum-free conditions may shed more light on the role of surface chemistry on the osteogenic differentiation of MPC (if there is any). It is entirely possible that the observed effects may be purely a result of the interplay between the charge and chemistry of the silica surface. However, in ongoing studies with various cell types, we have observed that NP modification promotes a high degree of order and density of F-actin fibers (unpublished data). This might suggest that NP modification enhances cell attachment, which in turn may diminish cell migration, thus favoring cell-differentiation functions. However, further studies are needed to elucidate which specific nanoscale-related factor (surface curvature or periodicity) plays a role in MPC growth and differentiation, with the potential to define new paradigms to control stem-cell function.

The surface-modification approach in this report is suitable for application to a wide range of biomaterials as it is independent of bulk characteristics. As NPs assemble into structures with long-range order, surface roughness can be influenced in a homogenous manner. By prefunctionalizing the NPs, both chemistry and roughness of metal and polymer surfaces can be modified predictably in a single step, and independently of each other. The observation that the lineage-specific differentiation of MPCs is enhanced on NP-modified surfaces in the presence of exogenous stimuli presents a unique avenue to influence function. By tethering cell-adhesion molecules and growth factors on the NP surface, biomolecular information can be co-localized with surface topography, thus allowing a rational design of biomaterial surfaces that promote or inhibit cell migration, a key process in inflammation and tissue-morphogenesis. Finally, the ability to vary texture and biomolecular information at the biomaterial/tissue interface in a spatially controlled manner may lend itself to nanoscale biomimetic engineering of biomaterial surfaces, which may be particularly suitable for directing the differentiation of stem cells into specific lineages.

Experimental

Preparation of NPs: The Stober process involves the controlled hydrolysis and condensation of an ethanolic solution of tetraethylorthosilicate, a silica precursor, in the presence of water and ammonium hydroxide.

50-nm NPs: Tetraethylorthosilicate (TEOS, 4.2 g in 50 mL of ethanol) was mixed with 2.5 g ammonia hydroxide and 1.2 g of deionized water, and the volume was adjusted to 100 mL using 200-proof ethanol.

100-nm NPs: 4.2 g TEOS in 50 mL of ethanol was mixed with 3.26 g ammonia hydroxide and 1.94 g of deionized water, and the volume was adjusted to 100 mL using 200-proof ethanol. The solution was stirred overnight to allow for coarsening of the NPs.

Aminosilation of the NP Surface: Amine functionality was introduced by reacting 50 ml of the NPs with 2 mL of APS at pH 4 (1 N acetic acid) for 1 h at room temperature followed by 3 h at 80 °C. The ANP suspension was cooled to room temperature and purified and concentrated by dialysis in ethanol. NP size and polydispersity was determined using dynamic laser-light scattering and the zeta potential (ζ) was measured using a ZetaSizer 3000HS (Malvern Instruments Ltd., Malvern, UK).

Preparation of Metal Polymer Substrates: Metals foils (0.05 mm, Goodfellow Corp. UK) were cut into rectangular pieces (1 cm × 0.7 cm), ultrasonically cleaned sequentially for 5 min in hexane, acetone, ethanol, and deionized water, and oven-dried at 60 °C for 24 h prior to use. PLA (Birmingham Polymers, Birmingham, Alabama, USA) thin films were spun from a 2 wt % solution in methylene chloride (100 μL; 3000 rpm; 22 s; 2 coats) onto ultrasonically cleaned borosilicate glass slide (ca. 1 cm × 1 cm) substrates.

NPs were assembled using spin-coating (2000 rpm, 20 s; 100 μL of NP suspension (1.8 w/v % in each deposition)■OK?■, total of 10 depositions, 1–2 min drying period between depositions). The modified metal substrates were heat-treated at 80 °C for 2 h under vacuum, whereas modified polymer samples were air-dried at room temperature.

Atomic Microscopy of NP-Modified Surfaces: Surfaces were mapped (Multimode AFM; Digital Instruments, USA) over a 1 μm × 1 μm area in tapping mode and the raw data was analyzed using Nanoscope III software package provided by the manufacturer. SEM images were obtained (JEOL 6300F FEG HRSEM) at an accelerating voltage of 10 keV and chamber vacuum of $3x10^{-6}$ torr (1 torr = 133.322 Pa).

Quantification of Amine Surface Functional Groups: Amine groups were quantified using the procedure detailed by Gaur et al. [21]. Substrates were first reacted at room temperature for 40 min with a sulfosuccinimidyl-4-*O*-(4,4′-dimethoxytrityl)-butyrate (Pierce, USA), a reagent that specifically reacts with primary amine groups. Subsequently, the reaction solution was aspirated and substrates were washed twice in 5 mL of Millipore deionized water and finally reacted with 2 mL of perchloric acid for 15 min to cleave the 4,4′-dimethoxytrityl cation (the molar extinction coefficient, $\varepsilon = 70\,000\ \mathrm{M}^{-1}\ \mathrm{cm}^{-1}$), which is measured at 498 nm.

Human Mesenchymal Progenitor Cell Studies

Cell Cultures: Human-bone-marrow aspirates from two independent donors were obtained during routine orthopedic surgical procedures involving exposure of the iliac crest, after informed patient consent, and in accordance with the local ethical commission (University Hospital, Basel). MPCs, generally also referred to as bone-marrow stromal cells or mesenchymal stem cells, were isolated as the adherent fraction of bone-marrow nucleated cells separated by Ficoll density centrifugation. Cells were expanded for two passages in complete medium (CM) supplemented with 5 $\mathrm{ng\,mL^{-1}}$ fibroblast growth factor 2 (FGF-2) and 10 nM dexamethasone [27]. CM consisted of α-minimum-essential medium (MEM) supplemented with 100 $\mathrm{\mu g\,mL^{-1}}$ streptomycin, 100 $\mathrm{\mu g\,mL^{-1}}$ penicillin, 10 % fetal bovine serum, 4.5 $\mathrm{mg\,mL^{-1}}$ D-Glucose, 0.1 mM nonessential Amino acids, 1 mM sodium pyruvate, 100 mM 4-(2-hydroxyethyl)-1-piperazineethanesulfonic acid (HEPES) buffer, and 0.29 $\mathrm{mg\,mL^{-1}}$ L-glutamine. Expanded MPCs were plated at a density of 3000 $\mathrm{cells\,cm^{-2}}$ on the metal sub-

strates, which were fixed on the bottom of six-well agarose-coated TCPS plates using a drop of fibrin glue. Cells were then differentiated by culture in osteogenic medium (OM), consisting of CM supplemented with 10 nM dexamethasone (Dex), 0.1 mM L-ascorbic acid 2-phosphate, and 10 mM β-glycerophosphate. Cultures were harvested after 7 and 14 days in OM, and assessed as described below.

DNA and Gene-Expression Assays: DNA amounts were measured in triplicate aliquots of cell layers scraped in 0.01 % sodium dodecyl sulfate (SDS), using the CyQUANT kit (Molecular Probes, Eugene, OR), with calf thymus DNA as a standard. In order to bypass the variability among cells from different donors, all values were reported as fold changes of the DNA amounts measured on TCPS at day 14 using cells from the same donor. Gene expression was quantified using real-time quantitative real-time polymerase chain reaction (RT-PCR) as previously described [27]. Briefly, RNA was extracted from cell layers using Trizol (Life Technologies, Basel, CH) according to the manufacturer's instructions, after sonication for 1 min. RNA was treated with the enzyme DNAse using the DNA-free Kit (Ambion, USA) and cDNA generated from using random hexamers (Catalys AG, CH) and Stratascript reverse transcriptase (Stratagene, NL) in the presence of dNTPs■please define—not all of our readers will know what this "standard" acronym stands for■. Using the ABI Prism 7700 Sequence Detection System (Applied Biosystems, Rotkreuz, CH), cDNA samples were analyzed both for the gene of interest (Bone Sialoprotein-2, BSP) and the housekeeping gene (18-S rRNA) using a multiplex approach (Perkin Elmer User Bulletin N. 2). RNA amounts of the gene of interest were normalized to the 18s rRNA, in order to derive the expression levels per cell [27], and reported as fold difference from those measured in cells of the same donor cultured in TCPS, in order to compensate for interindividual variability. Each sample was assessed at least in duplicate.

Received: December 6, 2005
Revised: September 26, 2006
Published online:■

[1] A. F. von Recum, T. G. van Kooten, *J. Biomater. Sci. Polym. Ed.* **1995**, *7*, 181.
[2] A. Itala, H. O. Ylanen, J. Yrjans, T. Heino, T. Hentunen, M. Hupa, H. T. Aro, *J. Biomed. Mater. Res.* **2002**, *62*, 404.
[3] M. Nitschke, G. Schmack, A. Janke, F. Simon, D. Pleul, C. Werner, *J. Biomed. Mater. Res.* **2002**, *59*, 632.
[4] S. Park, J. P. Bearinger, E. P. Lautenschlager, D. G. Castner, K. E. Healy, *J. Biomed. Mater. Res.* **2000**, *53*, 568.
[5] M. Lampin, R. Warocquier-Clerout, C. Legris, M. Degrange, M. F. Sigot-Luizard, *J. Biomed. Mater. Res.* **1997**, *36*, 99.
[6] P. N. Bartlett, P. R. Birkin, M. A. Ghanem, *Chem. Commun.* **2000**, 1671.
[7] A. Blanco, E. Chomski, S. Grabtchak, M. Ibisate, S. John, S. W. Leonard, C. Lopez, F. Meseguer, H. Miguez, J. P. Mondia, G. A. Ozin, O. Toader, H. M. van Driel, *Nature* **2000**, *405*, 437.
[8] P. Jiang, K. S. Hwang, D. M. Mittleman, J. F. Bertone, V. L. Colvin, *J. Am. Chem. Soc.* **1999**, *121*, 11 630.
[9] S. P. Massia, J. A. Hubbell, *J. Cell Biol.* **1991**, *114*, 1089.
[10] Surface topography was assessed as the root mean square (RMS) roughness (R_q) over a 1 μm^2 area. It is important to note that the RMS roughness as measured by using AFM may not reflect the actual surface roughness, as the AFM tip is incapable of accurately mapping regions deep in between two spherical bodies. However, the roughness values represent the general trends in the topography of the modified surfaces.
[11] The thickness of the NP assembly as accessed by Rutherford back scattering is in the range of 200–600 nm. Analysis of the metal-NP interface using a Focused Ion Beam (FIB) revealed a NP assembly around 300 nm in thickness (see Supporting Information for the microscopy image). The exact nature of interaction between the NP assembly and the material surface is unclear. Possible mechanisms of interaction include covalent binding with the metal oxide layer in the case of SS and Ti, and electrostatic interactions in the case of polymer surfaces. The NP assembly appears to be quite robust, is not damaged upon mechanical handling with SS tweezers, and is not easily scraped off using a doctor's blade under finger pressure.
[12] Upon modification of PLA spun-cast films with 100 nm NPs the R_q increased to (16.36 ± 0.72) nm, which is comparable to those seen on metal surfaces.
[13] A. Kumar, H. A. Biebuyck, G. M. Whitesides, *Langmuir* **1994**, *10*, 1498.
[14] R. D. Piner, J. Zhu, F. Xu, S. Hong, C. A. Mirkin, *Science* **1999**, *283*, 661.
[15] L. G. Cima, M. J. Cima, *US Patents 5 490 962* and *5 518 680*, **1996**
[16] J. Tan, H. Shen, W. M. Saltzman, *Biophys. J.* **2001**, *81*, 2569.
[17] H. Choi, I.-W. Chen, *J. Colloid Interface Sci.* **2003**, *258*, 435.
[18] The Stober process provides a very precise control over NP size and yields a monodisperse population, with a polydispersity (PD) of less than 0.1. Low PD is important to facilitate the formation of highly ordered NP assemblies that span the entire surface of a substrate. Upon aminosilation, the zeta potential (ζ) of the NP surface reversed from –30 mV to +27 mV at physiological pH of 7.4, as the surface is covered by protonated NH_2 groups.
[19] Y. N. Danilov, R. L. Juliano, *Exp. Cell Res.* **1989**, *182*, 186.
[20] G. Maheshwari, G. Brown, D. A. Lauffenburger, A. Wells, L. G. Griffith, *J. Cell Sci.* **2000**, *113*, 1677.
[21] R. K. Guar, K. C. Gupta, *Anal. Biochem.* **1989**, *180*, 253.
[22] Upon modification with ANP, the metal surfaces become positively charged [18]. As many of the proteins that promote cell adhesion such as fibronectin and vitronectin possess a net negative charge at physiological pH they might be expected to favorably interact with a positively charged amine surface thus enhancing cell attachment and proliferation.
[23] G. Decher, *Science* **1997**, *277*, 1232.
[24] The calorimetric assay involves the covalent binding of a dye-bearing heterofunctional molecule sulfo-succinimidyl-4-*O*-(4,4′-dimethoxytrityl)-butyrate (Sulfo-SDTB) to the amine group and then the subsequent cleavage of the dimethoxytrityl group to yield an orange colored solution that is assayed at 498 nm (the molar extinction coefficient, $\varepsilon = 70$ k M^{-1} cm^{-1}).
[25] M. Matsuzawa, P. Liesi, W. Knoll, *J. Neurosci. Methods* **1996**, *69*, 189.
[26] a) J. A. Schmidt, A. F. von Recum, *Biomaterials* **1992**, *13*, 1059. b) The role of cell shape in dictating cell function was first demonstrated by Folkman and Moscona in their seminal paper (A. Moscona, J. Folkman, *Nature* **1978**, *273*, 345).
[27] O. Frank, M. Heim, M. Jakob, A. Barbero, D. Schäfer, I. Bendik, W. Dick, M. Heberer, I. Martin, *J. Cell. Biochem.* **2002**, *85*, 737.
[28] These findings are in contrast to what has been observed by Lauer et al. [29], who found that the texture on the titanium surface (glossy-polished, sandblasted and plasma-sprayed) had no effect on proliferation of maxillar osteoblast-like cells. Similarly, Itala et al., found that the proliferation of human osteoblast-like cells (MG 63) on chemically roughened bioactive glass was similar to smooth substrates [2]. Our findings could therefore, have immense implications for surface engineering of implants to promote osseous integration.
[29] G. Lauer, M. Wiedmann-Al-Ahmad, J. E. Otten, U. Hubner, R. Schmelzeisen, W. Schilli, *Biomaterials* **2001**. *22*, 2799.

ADVANCED MATERIALS

COMMUNICATIONS

Biomedical Materials

A. M. Lipski, C. Jaquiery,
H. Choi, D. Eberli, M. Stevens,
I. Martin, I.-W. Chen,
V. P. Shastri* ..... ■ – ■

Nanoscale Engineering of Biomaterial Surfaces

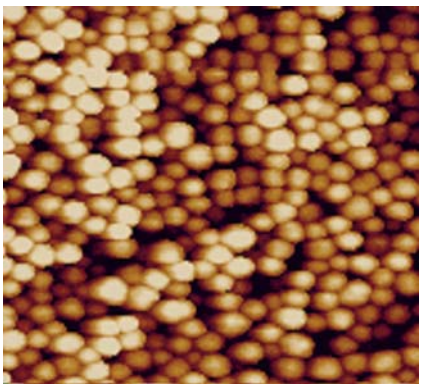

Single-step independent modification of the texture and chemistry of a material surface through the assembly of functionalized silica nanoparticles (NPs) is described. Such NP surface modifications enhance the differentiation of human-marrow-derived mesenchymal cells into an osteogenic lineage and present a new paradigm for nanoscale biomimetic engineering of a biomaterial surface.

